Radial askew endodermal cell divisions reveal IRK functions in division orientation

R. M. Imtiaz Karim Rony[1,2], Roya Campos[1], and Jaimie M. Van Norman[1,2]*

[1]Departments of Botany and Plant Sciences and [2]Molecular, Cell, and Systems Biology, Center for Plant Cell Biology, Institute of Integrative Genome Biology, University of California, Riverside, USA

***Corresponding Author:**
Jaimie M. Van Norman, jaimie.vannorman@ucr.edu

KEYWORDS
Arabidopsis root, development, cell division, division plane orientation, endodermis, cell polarity

SHORT TITLE (if needed)
IRK functions in cell division orientation (42 characters)

ABSTRACT

Oriented cell divisions produce different cell types and maintain tissue and organ patterning in plants; this is particularly true of the highly organized Arabidopsis root meristem. Because plant cells are encased by walls, the precise orientation of cell divisions is especially important for cell fate specification and tissue/organ organization. Mutant alleles of the transmembrane receptor kinase INFLORESCENCE AND ROOT APICES RECEPTOR KINASE (IRK) exhibit excess endodermal cell divisions, resulting in more cells in the radial axis of *irk* roots. IRK localizes to the outer polar domain of endodermal cells, which suggests directional signal perception is necessary to repress endodermal cell proliferation. Here, we conducted a detailed examination of endodermal cell divisions in *irk* and identified a distinct cell division orientation defect. Many excess endodermal divisions in *irk-4* have outwardly skewed division planes, therefore we termed them 'radial askew' divisions. An IRK truncation lacking the kinase domain retains polar localization and rescues these radial askew divisions, but exhibits excess periclinal divisions, phenocopying the weaker *irk-1* allele. These results expand IRK's function beyond repression of endodermal cell division activity showing it's also required for division plane orientation. Based on its polarity, we propose that IRK at the outer lateral endodermal cell face interferes with division plane selection, maintenance, and/or cell plate attachment to influence endodermal cell division orientation.

INTRODUCTION

In multicellular eukaryotes, cell division produces diverse cell types and increases cell numbers for body plan elaboration and growth. Cell divisions are typically categorized as proliferative (symmetric) and formative (asymmetric). Proliferative cell divisions are most often physically symmetrical, producing similarly sized daughter cells that share the same cell fate. In contrast, formative cell divisions produce different cell types. These divisions can be physically symmetrical or asymmetrical, but regardless of this, the daughter cells have distinct fates. Due to the cell wall, the relative position of individual plant cells is fixed in space; accordingly, cell division plane orientation is crucial in plant cell fate determination and tissue organization (Facette et al., 2018; Rasmussen and Bellinger, 2018). Thus, in plants, the developmental trajectory of a daughter cell is influenced by division plane orientation indicating this is a key developmental decision.

The orientation of plant cell divisions is described by how the new cell wall is positioned relative to the surface of the organ (Livanos and Müller, 2019). Regardless of the organ,

periclinal cell divisions are oriented parallel to the surface and anticlinal cell divisions are oriented perpendicular to the surface. For anticlinal cell divisions, the division plane can be aligned with the organ's longitudinal or transverse axis (Figure 1A, B); therefore, we distinguish between longitudinal anticlinal and transverse anticlinal cell divisions. In the root, periclinal cell divisions are often formative as they generate additional layers of distinct cell types (De Smet and Beeckman, 2011; Pillitteri et al., 2016). In contrast, anticlinal cell divisions in the root are typically proliferative, generating more cells of the same type. Normal tissue and organ patterning require the specific orientation of proliferative and formative cell divisions relative to the plant body axis. Yet our understanding how division orientation and frequency are precisely controlled remains limited.

The highly stereotypical cellular organization of the *Arabidopsis thaliana* root makes it an ideal system in which to investigate how the frequency and orientation of cell division contributes to tissue/organ patterning. Root cell division planes that deviate from the three typical orientations lead to irregular daughter cell shapes and, thus, the consequences of any misoriented divisions can be followed in time and space. In the root, precisely oriented cell divisions contribute to the general organization of root tissues as a set of nested cylinders with individual initial cells (stem cells) giving rise to specific cell types or lineages (Dolan et al., 1993; Van Norman, 2016; Scheres and Benfey, 1999). In the root's longitudinal axis, cell types are present in linear files extending shootward from the quiescent center and stem cells (Figure 1). In the transverse axis, the outer cell layers of epidermis, cortex, and endodermis form concentric rings of cells around the central stele, which contains the pericycle and the plant vascular tissues. This organization is established in the plant embryo and maintained in the root meristem post-embryonically through strict cell division control.

The formation of the cortex and endodermis, collectively, the root ground tissue (GT), is a good example of how a specific series of oriented formative cell divisions give rise to the distinct cell types. First, the GT stem cell, the cortex/endodermal initial (CEI, Figure 1A, B), undergoes a formative, transverse anticlinal division to produce a daughter cell. This daughter cell then undergoes a formative, periclinal cell division to produce endodermis towards the inside and cortex cells towards the outside (Figure 1B, (Dolan et al., 1993; Scheres and Benfey, 1999). As the plants get older, endodermal cells can undergo another periclinal division to produce a second cortex layer called middle or secondary cortex (Paquette and Benfey, 2005;

Cui, 2016). Thus, specifically oriented, formative cell divisions produce each root ground tissue cell type.

After their formation, cortex and endodermal cells proliferate through symmetrical, transverse anticlinal divisions producing more cells in their respective longitudinal files. Symmetrical, longitudinal anticlinal cell divisions can also occur and would produce more GT cells in the root's radial axis (Figure 1A). However, these divisions are not often observed in the root and, as a result, eight of each GT cell type, including the CEI, are most often observed in the root's radial axis (Dolan et al., 1993; Scheres and Benfey, 1999). This strict regulation of root GT cell number in the radial axis is disrupted in mutant alleles of IRK (INFLORESCENCE AND ROOT APICES RECEPTOR KINASE), which exhibit excess longitudinal anticlinal and periclinal cell divisions in the endodermis (Campos et al., 2020). These excess cell divisions coincide with promoter activity of a specific D-type cyclin, *CYCLIN D6;1* (Campos et al., 2020), which suggests that longitudinal anticlinal and periclinal endodermal cell divisions are developmentally regulated and have common control elements downstream of IRK.

IRK encodes a transmembrane receptor kinase of the Arabidopsis RECEPTOR-LIKE KINASE (RLK) super family (Shiu and Bleecker, 2001, 2003). IRK accumulates to the outer polar domain of the endodermal plasma membrane. Although IRK is expressed broadly in root cell types, endodermal-specific expression of IRK is sufficient to rescue the cell division defects, suggesting that IRK function is particularly important for repression of endodermal cell division activity (Rodriguez-Furlan et al., 2022; Campos et al., 2020). Unexpectedly, and unlike other receptor kinases in plant and animal systems, IRK maintains its polar localization even when the intracellular domain is deleted and this truncated version of the protein remains partially functional rescuing the endodermal LADs but not the periclinal divisions (Rodriguez-Furlan et al., 2022). Polar accumulation of IRK to the outer lateral face of endodermal cells together with its function in repression of endodermal cell proliferation in the radial axis suggest that perception of an extracellular cue, likely originating in cells peripheral to the endodermis, by IRK is required to maintain GT cell number post-embryonically. However, the molecular details of IRK function remain unknown.

Here, we closely examined the excess endodermal divisions in *irk* mutants and identified a distinct cell division orientation defect. Unexpectedly in *irk-4,* a null allele, the majority of endodermal cell divisions previously characterized as periclinally oriented are, instead,

misoriented with outwardly skewed division planes. We define these as radial askew divisions, because the new cell plate obliquely divides cells producing small, abnormally shaped cells peripheral to the endodermis. Unexpectedly, in the weaker *irk-1* allele, roots do not show excess radial askew endodermal cell divisions, but have excess longitudinal anticlinal and periclinal divisions. An IRK intracellular truncation rescues the radially askew endodermal divisions in *irk-4*, but excess periclinal divisions are present, phenocopying *irk-1*. These results expand the function of IRK beyond repression of endodermal cell division activity to include a requirement for it in cell division plane orientation. Given its polar accumulation in the plasma membrane, IRK may participate in division plane orientation through physical involvement with cell plate orientation and/or attachment. We propose a model whereby the presence of IRK at the outer polar domain occludes that endodermal cell face for division plane selection or cell plate attachment.

RESULTS

Many endodermal cell divisions in *irk-4* are abnormally oriented

In the endodermis, proliferative cell divisions occur in the transverse anticlinal orientation, producing more cells per endodermal file. The Arabidospis endodermis can also undergo periclinal divisions to produce another layer of ground tissue, which becomes the middle or secondary cortex layer (Figure 1B). In Wild type, this second layer of cortex is typically formed later, as plants mature. In the wild type endodermis, divisions in the longitudinal anticlinal orientation, which generate more cells per ring, occur relatively infrequently. In contrast, in *irk-4* roots, we observed periclinal divisions occurring earlier than wild type and many longitudinal anticlinal cell divisions (Campos et al., 2020; Rodriguez-Furlan et al., 2022). No increase in transverse anticlinal (proliferative) divisions were observed in *irk-4*, suggesting IRK specifically represses cell division activity that produces cells in the root's radial axis.

Close examination of GT cell division orientation in *irk-4* revealed that divisions we had previously classified as periclinal were not actually oriented parallel to the root's surface. If considered in 2-dimensions (2D), upon completion of a periclinal division, the new cell plate fuses at sites on opposite endodermal cell faces within a cell file. However, in *irk-4,* we observed misoriented divisions where cell plates appeared to fuse at a shoot/rootward and outer lateral endodermal face (Fig 1C, D). Cell plate fusion sites on adjacent cell faces are abnormal, failing to orient parallel or perpendicular to the surface of the root. This oblique division plane orientation results in these divisions often appearing to be periclinally oriented when viewed only

in the median longitudinal section. However, in a series of longitudinal and transverse sections (in confocal z-stacks (Campos and Van Norman, 2022)), the key differences between periclinal and these misoriented divisions is clear. Additionally, periclinal divisions bisect endodermal cells in half whereas the misoriented divisions divide endodermal cells at an angle resulting in smaller daughter cells that are somewhat prism shaped. We termed these radial askew endodermal divisions and they reveal additional phenotypic consequences of loss of IRK function.

To assess the frequency of these divisions, we re-examined a previous image-set (Rodriguez-Furlan et al., 2022) to specifically parse radial askew divisions from those oriented periclinally. Reassessment of these images revealed that 88.8% of the divisions we classified as periclinal in *irk-4* (n = 224 divisions) were actually radial askew divisions. This showed that there was no significant difference in the number of periclinal divisions in *irk-4* compared to wild type (Figure 1F). In young wild type roots, periclinal divisions are somewhat rare, yet 5.1% of the divisions we classified as periclinal (n = 59 divisions) were radial askew. In *irk-1*, a partial loss of function allele, we found that 15.6% of divisions classified as periclinal (n = 154 divisions) are radial askew oriented. Despite this, *irk-1* roots continue to have significantly more periclinal divisions than wild type (Figure 1F). These analyses revealed key phenotypic differences between these *irk* alleles. Namely *irk-4* has significantly more radial askew and longitudinal anticlinal divisions than wild type, whereas *irk-1* has significantly more radial askew and periclinal divisions, but the overall numbers of excess radial askew endodermal divisions in *irk-1* are not as numerous as in *irk-4*. These results indicate that IRK functions not only to repress endodermal cell division activity but also participates in cell division plane orientation.

Distinct cell division orientation defects occur among *irk* alleles

Based on the genetic lesions of the *irk* alleles, *irk-4* is a presumptive null allele, while *irk-1* is a partial loss of function allele (Campos et al., 2020). *irk-1* results from the insertion of T-DNA near the beginning of the coding region for the kinase domain. We previously showed that GFP fused to a truncated version of IRK missing its kinase domain (IRKΔK-GFP) is polarly localized in the endodermis and, while it fully rescued the *irk-4* endodermal longitudinal anticlinal division (LAD) phenotype, it did not rescue the periclinal division phenotype (Rodriguez-Furlan et al., 2022). This is similar to the *irk-1* cell division phenotype and therefore, is consistent with production of a truncated, partially functional version of IRK that results in a milder cell division phenotype.

With the detection of novel phenotypic consequences of *irk* loss of function, we investigated whether IRKΔK could rescue the radial askew cell division phenotype of *irk-4*. We found that *irk-4* roots expressing either the full-length version of IRK-GFP or IRKΔK-GFP showed rescue of the endodermal LAD and radial askew phenotypes (Figure 1H). Unexpectedly, *irk-4* expressing IRKΔK-GFP showed significantly more periclinal endodermal divisions than wild type or *irk-4* IRK-GFP plants, similar to *irk-1* roots. This indicates that the presence of IRKΔK at the outer polar domain of the endodermis is sufficient to repress longitudinal anticlinal and radial askew divisions in *irk-4*. Therefore, while there are still excess endodermal divisions in *irk-4* IRKΔK-GFP roots, they are predominantly periclinally oriented suggesting the kinase domain is largely dispensable for IRK's role in division plane orientation, but participates in repression of cell division activity.

Radial askew endodermal cell divisions in *irk-4* coincide with *CYCD6;1* promoter activity

In wild type roots, formative ground tissue cell divisions are associated with promoter activity of specific D-type cyclin, *pCYCD6;1*, this includes divisions of the initial cells and periclinal endodermal divisions to form middle cortex (Sozzani et al., 2010). In *irk* mutants, we found that endodermal LADs also coincide with activity of *pCYCD6;1* (Campos et al., 2020). Based on our initial *irk* analyses, we proposed longitudinal anticlinal and periclinal division orientations share some common regulatory mechanism(s) downstream of IRK.

Due to the identification of radial askew cell divisions from the population of excess endodermal divisions in *irk-4*, we conducted a detailed examination of *pCYCD6;1:erGFP* expression in *irk* and wild type roots (Figure 2). As we previously reported, *pCYCD6;1* activity is substantially increased in the *irk* endodermis compared to wild type Figure 2A, B). We quantified the abnormal endodermal cell divisions together with expression of *pCYCD6;1:erGFP* and mapped this information in the root's longitudinal axis (Figure 2B, C). In wild type, endodermal LADs occur much less frequently than in *irk* mutants and we rarely see these daughter cells associated with *pCYCD6;1* activity (Figure 2B, C). This is consistent with repression of a cell cycle reporter that is temporally restricted during cell division. More endodermal LADs are observed in *irk-1* than wild type and the daughter cells frequently show *pCYCD6;1* activity. Under these conditions, *irk-4* roots have endodermal LADs at nearly every position in the longitudinal axis and, with rare exception, these daughter cells express *pCYCD6;1:erGFP* (Figure 2C). These results reveal extensive excess endodermal LADs in *irk* and confirm their association with *pCYCD6;1* activity.

To determine whether radial askew endodermal cell divisions were also associated with *pCYCD6;1* activity, we mapped them onto the root's longitudinal axis (Figure 3). When radial askew divisions are observed in the wild type endodermis, they are consistently associated with *pCYCD6;1* activity (Figure 3B, C). This was also observed in *irk* mutants, which had many more radial askew endodermal divisions (Figure 3B). In wild type and *irk-1* these divisions begin to occur five or more cells above the quiescent center (QC), however in *irk-4,* radial askew divisions occur much more frequently and closer to the QC (Figure 3C). Like endodermal LADs, the daughter cells of radial askew divisions are nearly always coincident with *pCYCD6;1* activity. Altogether, our endodermal cell division maps reveal extensive abnormal endodermal cell divisions, particularly in *irk-4,* and show consistent *pCYCD6;1* activity in the daughter cells of LADs and radial askew divisions. Thus, *pCYCD6;1* activity is associated with all of the excess endodermal cell divisions observed in *irk* and implicate IRK in repression of cell cycle activity in the endodermis.

The peripheral daughter cells of radial askew endodermal divisions in *irk-4* express a marker of cortex identity

Endodermal periclinal, longitudinal anticlinal, and radial askew cell divisions result in an increase in the number of ground tissue cells in the *irk* root's radial axis. LADs produce more endodermal cells around the stele, while periclinal divisions produce another GT layer, the middle cortex. As endodermal radial askew cell divisions produce prism-shaped cells of unknown identity that are peripherally located, we examined expression of reporter genes of endodermal and cortex cell identities (Figure 4). We first examined *SCARECROW* promoter activity (*pSCR:erGFP*), which is expressed in endodermal cells throughout the root (Wysocka-Diller et al., 2000; Di Laurenzio et al., 1996). In wild type, most of the peripheral daughters of radial askew divisions do not show *pSCR* activity. In *irk-1*, these daughter cells most often show *pSCR* activity and in *irk-4*, about 60% of these daughters show *pSCR* activity (Figure 4B, C). This suggests that these daughter cells are not maintaining *pSCR* activity implying they may be transitioning away from endodermal identity.

Next, we examined a reporter for cortex identity, *CORTEX2* promoter driving nuclear localized-yellow fluorescent protein (*pCO2:nlsYFP*), which is expressed in meristematic cortex cells. In wild type roots, cells immediately peripheral to the endodermis have cortex identity, whether those cells are derived from periclinal CEID or endodermal divisions (Figure 1B). In

irk-4 we observe that ~20% of the peripheral daughters of radial askew divisions exhibit *pCO2* activity (Figure 4E, F). Comparison of the activity of *pSCR* and *pCO2*, particularly in *irk-4*, suggests that the peripheral daughters of endodermal radial askew divisions gradually acquire cortex cell fate similar to what is observed for the daughter cells of periclinal endodermal divisions.

Radial askew and periclinal endodermal divisions often co-occur in the longitudinal axis

Typically root cell divisions bisect cells strictly with respect to the root's surface. When considered in 2D, periclinal endodermal divisions occur when a new cell plate attaches to the rootward and shootward endodermal faces and LADs occur when the new cell plate attaches to the outer and inner endodermal faces. Each of these divisions produces similarly sized daughter cells. In contrast, radial askew divisions are oblique and create smaller prism-shaped cells that are peripherally positioned. When considered in 2D, radial askew endodermal divisions occur when a new cell plate attaches to the outer lateral endodermal face and an adjacent root-/shootward endodermal face. Thus, one cell plate attachment face is shared with one of the attachment faces observed in each longitudinal anticlinal and periclinal endodermal cell divisions (Figure 5A). This led us to ask whether radial askew divisions were correlated with either periclinal or LADs in the longitudinal axis.

Within endodermal cell files, we identified cells that had undergone radial askew division and determined whether the adjacent (shootward and/or rootward) cell had divided and how that division was oriented (Figure 5B, C). In wild type, endodermal cells that have undergone radial askew divisions the shootward and/or rootward neighbor had divided periclinally about half of the time (Figure 5D). Otherwise the neighbor had not divided at all. In *irk-1,* radial askew endodermal divisions were adjacent to a periclinal division >60% of the time. In *irk-4*, radial askew divisions were most often adjacent to endodermal cells that had not divided, to periclinal divisions just over 25% of the time, and were rarely flanked by LADs (Figure 5D). Given that endodermal radial askew divisions are rare in wild type their co-occurrence with periclinal division is striking. Likewise in *irk-4*, it is surprising that radial askew divisions are most often adjacent to endodermal cells that have not divided or have undergone a periclinal division, given that endodermal LADs are extremely numerous. These results suggest that, regardless of genotype, endodermal radial askew divisions are most often adjacent to cell that have divided periclinally or not divided at all. Given that the daughter cells of endodermal radial askew divisions are peripherally located, begin to express a cortex marker, and their neighbors are

more likely to have divided periclinally, we conclude the radial askew divisions are likely misoriented periclinal divisions.

DISCUSSION

We have identified radial askew endodermal cell divisions in *irk* mutants, a novel aspect of their mutant phenotype. The results show that IRK functions not only in endodermal cell division activity, but is also required for cell division orientation. Typically endodermal cell division orientations bisect cells with respect to the root's surface, however, radial askew divisions are oblique and create small prism shaped cells that are more peripherally positioned. When considered in 2D, radial askew endodermal divisions occur when a new cell plate attaches to the adjacent outer lateral endodermal face and a root-/shootward endodermal face. Thus, they share one attachment face with both longitudinal anticlinal and periclinal endodermal cell divisions. It is possible that radial askew endodermal divisions arise from misorientation of one edge of the cell plate during what would have been a longitudinal anticlinal or periclinal endodermal division. We show that radial askew divisions are spatially correlated with periclinal divisions in all genotypes, suggesting they are misoriented periclinal divisions.

We were particularly surprised to observe that the smaller daughter cells of radial askew endodermal divisions were invariably positioned peripherally - nearer the cortex. If these skewed divisions were the result of random placement of new cell plates, we would expect that approximately half would attach at the inner lateral endodermal face, such that the smaller daughter cells were positioned towards the interior - nearer the pericycle. Because this was not observed in any of our experiments, there is no support for random cell division plane placement in *irk-4.* Instead, our observations suggest that some positional information remains to orient the new cell division planes away from this cell face.

The specific orientation of radial askew endodernal divisions together with the differences in division orientation based on the IRK genotype suggests that endodermal division activity and orientation are specifically regulated. One possible explanation for these observations is partitioning of function across the IRK protein domains. For instance, if the kinase domain were important for repressing endodermal cell division activity, then we would expect to observe comparable increases in excess endodermal cell divisions in *irk-4* and *irk-1,* because the kinase domain is absent in both of these genotypes. However, in *irk-1* roots, where the IRK extracellular and transmembrane domains are likely intact and only the kinase domain

is missing, there are many fewer (~4x less) abnormal endodermal divisions than in *irk-4*. This suggests that the IRK extracellular and/or transmembrane domains are also important for its function to repress endodermal cell division activity. Interestingly, the IRK extracellular and/or transmembrane domains are necessary for its polar accumulation at the plasma membrane, while the kinase domain is dispensable for its polarity (Rodriguez-Furlan et al., 2022). Therefore, the IRK domains responsible for its polarity are also required for the majority of its function in repression of endodermal cell division activity.

A role for IRK in both of these processes is particularly compelling when the spatial relationship between cell division orientations in *irk* and IRK polar accumulation is considered (Figure 6). In *irk-4,* significant increases are observed only for radial askew or longitudinal anticlinal endodermal divisions and for each of these, one edge of the division plane attaches to the outer lateral endodermal face. This coincides with where full-length IRK and IRKΔK localize (Figure 6A, B). Thus, in the *irk-1* or *irk-4* IRKΔK-GFP endodermis, where a portion of IRK is present at the PM, we observe fewer radial askew and LADs and more periclinal divisions than in *irk-4*. In this situation, the increased endodermal cell divisions are oriented such that the new cell plate does not contact the outer lateral endodermal cell face. This leads to the hypothesis that the presence of IRK or IRKΔK on this cell face inhibits attachment of new cell plates. This is consistent with the *irk-4* endodermal cell division phenotype where higher numbers of abnormal endodermal cell divisions occur with many of the newly formed cell plates attaching to the outer lateral endodermal face and leading to broader defects in GT tissue patterning.

The extensive activity of *pCYCD6;1* in *irk* roots may simply reflect the high number of endodermal cell divisions occurring at any one time, however, it is also possible that spatiotemporal suppression of cell cycle activity in *irk* is generally defective. This would lead to persistent expression of cell cycle genes after cytokinesis and could partially explain the excess endodermal cell divisions observed in *irk* mutants. However, there is no increase in transverse anticlinal endodermal division in *irk-4*, rather IRK represses particular endodermal cell divisions, which ultimately, broaden the root's radial axis, by generating more cells around the stele or more layers of GT (Campos et al., 2020). This suggests that division orientations that broaden the GT in the radial axis share common regulatory elements downstream of IRK and may involve specific cell cycle components, like CYCD6;1. As neither IRK nor CYCD6;1 have any known roles in proliferative, transverse anticlinal endodermal cell divisions (Sozzani et al., 2010; Campos et al., 2020), it suggests regulation of these divisions occurs through a distinct

mechanism. The idea that plant cells might separately regulate divisions occurring in distinct orientations would make cell division regulation, including division plane establishment and maintenance, and the execution of cytokinesis, much more complex, however our data suggest we should be open to that possibility.

The orientation of the IRK-repressed endodermal cell divisions and its lateral polarity suggest a direct link between IRK polarity and cell plate orientation. To instruct cell division plane orientation, polarly localized proteins must, ultimately, influence positioning of cell division machinery. In plant cells, this includes the mitotic spindle and two plant-specific cytoskeletal structures, the preprophase band, which participates in establishing the division plane, and the phragmoplast, which assembles and guides the new cell plate formation. There is increasing evidence, particularly from the stomatal development literature, that polarity domains with a cell can directly and/or indirectly position these structures via linkage with the cytoskeleton. For example, the BASL/BRX family polarity domain depletes cortical microtubules at particular positions to ensure the preprophase band forms outside the site marked by the polarity domain (Muroyama et al., 2022). Additionally, the *trm6,7,8* triple mutant, which does not form preprophase bands, exhibits minor root cell division defects and fails to pattern stomata correctly as the links between cell polarity and division orientation are disrupted (Schaefer et al., 2017). Identification of the links between IRK and cell division mechanics are key avenues of future investigation and will expand our knowledge of the precise mechanisms underlying cell division activity and orientation.

MATERIALS & METHODS

Plant material and growth conditions

Seeds were surface sterilized with chlorine gas and plated on MS agar media. The media contained 0.2X Murashige and Skoog salts (Caisson labs), 0.5g/L MES, 1% Sucrose, and 1% agar (Difco) and was at pH 5.7. Plates were sealed with parafilm and placed at 4˚C for 24-72 hours for stratification. After stratification, plates were placed vertically in a Percival incubator and grown under 16 hrs light/8hrs dark at a constant temperature of 22˚C. For each experiment, the genotypes being analyzed were grown side-by-side on the same plate. *Arabidopsis thaliana* ecotype Col-0 was used as the Wild Type. The genotypes *irk-1*, *irk-4*, *irk-4 pIRK:IRKΔK:GFP*, and *irk-4 pIRK:IRK:GFP* were obtained as previously described (Campos et al., 2020; Rodriguez-Furlan et al., 2022). The cell type specific reporters *pCO2:nlsYFP (Paquette and Benfey, 2005)*, *pSCR:erGFP (Wysocka-Diller et al., 2000; Di Laurenzio et al.,*

1996), and *pCYCD6;1::GUS:GFP* (Sozzani et al., 2010) were received from the Benfey lab and were crossed the *irk* mutants as previously described (Campos et al., 2020).

Confocal microscopy and image analysis

Roots were imaged at day 6 post-stratification (dps) and stained with ~10 μM propidium iodide (PI) solubilized in water for 1-2 minutes; then imaged on a Leica SP8 upright microscope and imaging system housed in the Van Norman lab. The pinhole was set to 1-1.2 airy units and the fluorescent signals were captured using the following settings: PI (excitation 536 nm, emission 585-660 nm) and GFP/YFP (excitation 488 nm, emission 492-530 nm). Z-stacks were acquired and analyzed with the orthogonal sectioning tool of the LASX software. The total number of endodermal divisions per root were counted from the QC to QC+120μm or 20 cells as previously described (Campos and Van Norman, 2022).

Representative images of roots expressing the *pCYCD6;1:erGFP*, *pSCR:erGFP* and *pCO2:nls:YFP* reporters were acquired from a transverse section at the 10th endodermal cell (ED 10) shootward of the QC.

For the images used to quantify abnormal endodermal cell divisions and generate the endodermal cell division map (see below), Z-stacks were acquired from each root at 512×512 pixels with 1 μm between optical sections. All three genotypes expressing a single reporter were grown on the same plate, 14-15 plants per genotype were imaged, and ≥10 plants per genotype were analyzed in detail. For each root, the optical sections were manually analyzed from the QC shootward 20 endodermal cells (ED 1-20), such that >160 endodermal cells per root were examined for abnormal cell divisions.

Generation of the endodermal cell division maps

To generate the endodermal cell division maps for each genotype, we examined promoter activity and the presence of abnormal (periclinal, radial askew, or longitudinal anticlinal) divisions from the QC shootward to endodermal cell position 20. If an endodermal cell had an abnormal division, we documented whether the daughter cell is positive or negative for a given reporter. For plants expressing *pCYCD6;1:erGFP*, we examined endodermal LADs, periclinal and radial askew divisions. For; plants expressing *pSCR:erGFP* and *pCO2:nls:YFP*, we only examined the endodermal periclinal and radial askew divisions, as the daughters of endodermal LADs are expected to remain endodermal cells. The total number of abnormal

divisions was quantified per root and then counted as GFP/YFP positive (+) or GFP/YFP negative (-).

The endodermal cell division map shows whether an abnormal division was present in a root's longitudinal axis at any of the analyzed positions (ED 1 to ED 20). However, this information is compressed and does not include the number of divisions or division mapping in the radial axis. Specifically, if a box within the division map is a solid color, then all of the daughter cells resulting from an abnormal division were expressing the reporter - whether there was a single abnormal division or many. If some (but not all) of the daughter cells were expressing the reporter, then the box has a gradient fill. Finally, if none of the daughter cells expressed the reporter then the box is white. Endodermal LADs are indicated by a black arrowhead on the right, internal side of each box, periclinal divisions are indicated by a black arrowhead on the lower, internal side of each box, and radial askew divisions are indicated by a curved line in the lower-right corner of each box. If no abnormal endodermal cell division was detected, the box is empty and white.

Figure generation

Confocal images were exported from Leica software (LASX) as TIF files, which were cropped and resized in Adobe Photoshop. Graphs were generated with PRISM8 (GraphPad software https://www.graphpad.com/, San Diego, USA). Schematics were created in Adobe Illustrator. The figures containing confocal images, graphs, and schematics were all assembled in Adobe Illustrator.

ACKNOWLEDGEMENTS

We thank former members of the Van Norman lab including Jason Goff, Jessica N. Toth, and Cecilia Rodriguez Furlan for discussions of and feedback on this manuscript while it was in preparation. We also thank Patricia Springer for her insightful suggestion on how to display the endodermal division map. We appreciate access to the Institute of Integrative Genome Biology Microscopy Core Facility (UC, Riverside).This work was supported by Initial Complement (IC) funds from the University of California, Riverside, USDA-NIFA-CA-R-BPS-5156-H and NSF CAREER award #1751385 to J.M.V.N.

AUTHOR CONTRIBUTIONS

Conceptualization: RC and JMVN; Cell division methodology: RC and JMVN; Endodermal division & FP mapping: RMIKR and RC; Resources: JMVN and RC.; Writing - Original Draft and

Review and Editing: JMVN, RC, RMIKR; Visualization: RMIKR, RC, and JMVN.; Supervision: JMVN; Funding Acquisition: JMVN.

REFERENCES

Campos, R., Goff, J., Rodriguez-Furlan, C., and Van Norman, J.M. (2020). The Arabidopsis Receptor Kinase IRK Is Polarized and Represses Specific Cell Divisions in Roots. Dev. Cell **52**: 183–195.e4.

Campos, R. and Van Norman, J.M. (2022). Confocal Analysis of Arabidopsis Root Cell Divisions in 3D: A Focus on the Endodermis. Methods Mol. Biol. **2382**: 181–207.

Cui, H. (2016). Middle Cortex Formation in the Root: An Emerging Picture of Integrated Regulatory Mechanisms. Mol. Plant **9**: 771–773.

De Smet, I. and Beeckman, T. (2011). Asymmetric cell division in land plants and algae: the driving force for differentiation. Nat. Rev. Mol. Cell Biol. **12**: 177–188.

Di Laurenzio, L., Wysocka-Diller, J., Malamy, J.E., Pysh, L., Helariutta, Y., Freshour, G., Hahn, M.G., Feldmann, K.A., and Benfey, P.N. (1996). The SCARECROW gene regulates an asymmetric cell division that is essential for generating the radial organization of the Arabidopsis root. Cell **86**: 423–433.

Dolan, L., Janmaat, K., Willemsen, V., Linstead, P., Poethig, S., Roberts, K., and Scheres, B. (1993). Cellular organisation of the Arabidopsis thaliana root. Development **119**: 71–84.

Facette, M.R., Rasmussen, C.G., and Van Norman, J.M. (2018). A plane choice: coordinating timing and orientation of cell division during plant development. Curr. Opin. Plant Biol. **47**: 47–55.

Livanos, P. and Müller, S. (2019). Division Plane Establishment and Cytokinesis. Annu. Rev. Plant Biol. **70**: 239–267.

Muroyama, A., Gong, Y., Hartman, K.S., and Bergmann, D. (2022). Cortical polarity ensures its own asymmetric inheritance in the stomatal lineage to pattern the leaf surface. bioRxiv: 2022.07.15.500234.

Paquette, A.J. and Benfey, P.N. (2005). Maturation of the ground tissue of the root is regulated by gibberellin and SCARECROW and requires SHORT-ROOT. Plant Physiol. **138**: 636–640.

Pillitteri, L.J., Guo, X., and Dong, J. (2016). Asymmetric cell division in plants: mechanisms of symmetry breaking and cell fate determination. Cell. Mol. Life Sci.

Rasmussen, C.G. and Bellinger, M. (2018). An overview of plant division-plane orientation. New Phytol. **219**: 505–512.

Rodriguez-Furlan, C., Campos, R., Toth, J.N., and Van Norman, J.M. (2022). Distinct mechanisms orchestrate the contra-polarity of IRK and KOIN, two LRR-receptor-kinases controlling root cell division. Nat. Commun. **13**: 235.

Schaefer, E., Belcram, K., Uyttewaal, M., Duroc, Y., Goussot, M., Legland, D., Laruelle, E., de Tauzia-Moreau, M.-L., Pastuglia, M., and Bouchez, D. (2017). The preprophase band of microtubules controls the robustness of division orientation in plants. Science **356**: 186–189.

Scheres, B. and Benfey, P.N. (1999). ASYMMETRIC CELL DIVISION IN PLANTS. Annu. Rev. Plant Physiol. Plant Mol. Biol. **50**: 505–537.

Shiu, S.H. and Bleecker, A.B. (2003). Expansion of the receptor-like kinase/Pelle gene family and receptor-like proteins in Arabidopsis. Plant Physiol. **132**: 530–543.

Shiu, S.H. and Bleecker, A.B. (2001). Receptor-like kinases from Arabidopsis form a monophyletic gene family related to animal receptor kinases. Proc. Natl. Acad. Sci. U. S. A. **98**: 10763–10768.

Sozzani, R., Cui, H., Moreno-Risueno, M.A., Busch, W., Van Norman, J.M., Vernoux, T., Brady, S.M., Dewitte, W., Murray, J.A.H., and Benfey, P.N. (2010). Spatiotemporal regulation of cell-cycle genes by SHORTROOT links patterning and growth. Nature **466**: 128–132.

Van Norman, J.M. (2016). Asymmetry and cell polarity in root development. Dev. Biol. **419**: 165–174.

Wysocka-Diller, J.W., Helariutta, Y., Fukaki, H., Malamy, J.E., and Benfey, P.N. (2000). Molecular analysis of SCARECROW function reveals a radial patterning mechanism common to root and shoot. Development **127**: 595–603.

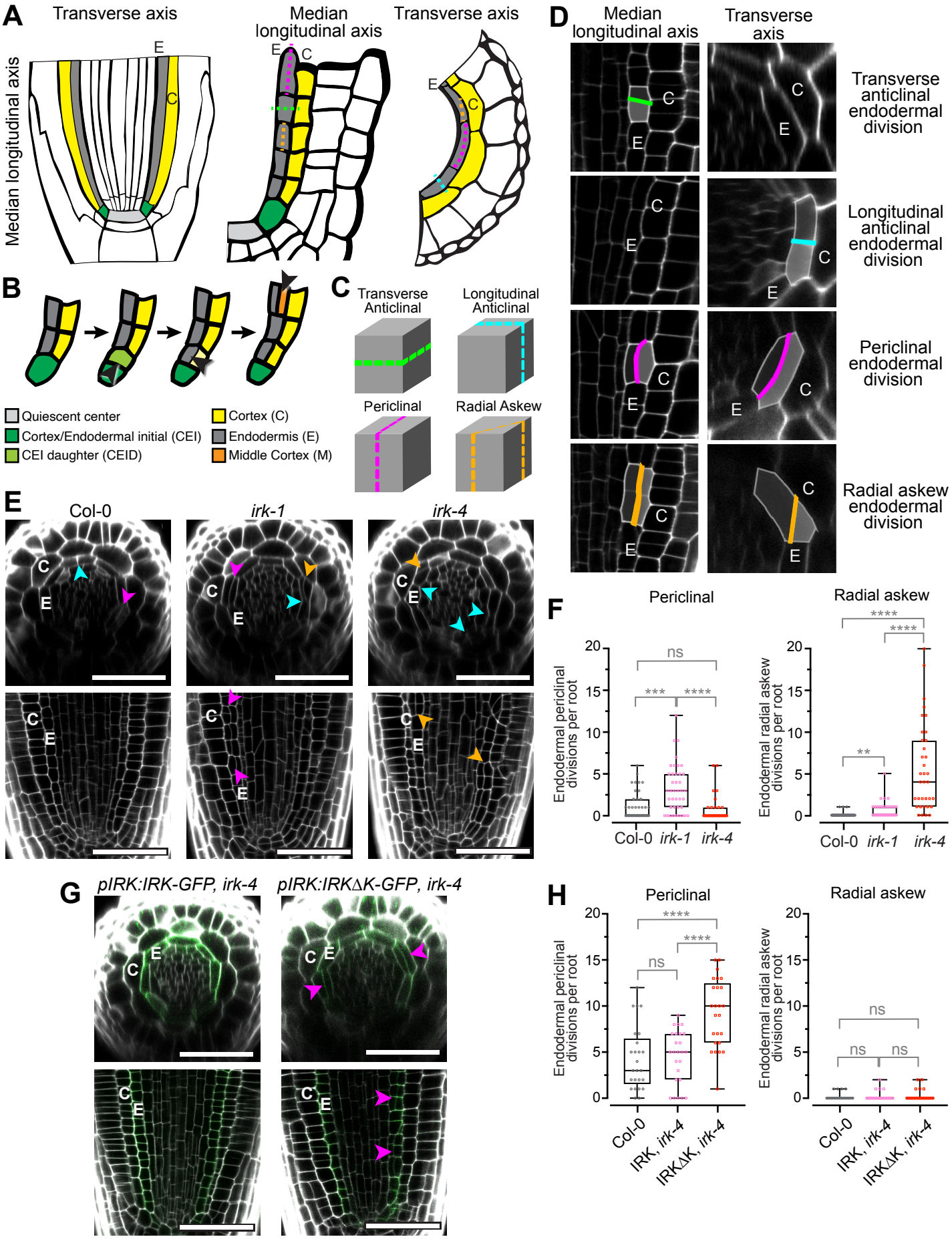
A
Transverse axis
Median longitudinal axis
Transverse axis
Median longitudinal axis
E
C
B
Quiescent center
Cortex/Endodermal initial (CEI)
CEI daughter (CEID)
Cortex (C)
Endodermis (E)
Middle Cortex (M)
C
Transverse Anticlinal
Longitudinal Anticlinal
Periclinal
Radial Askew
D
Median longitudinal axis
Transverse axis
Transverse anticlinal endodermal division
Longitudinal anticlinal endodermal division
Periclinal endodermal division
Radial askew endodermal division
E
Col-0
irk-1
irk-4
F
Periclinal
Radial askew
Endodermal periclinal divisions per root
Endodermal radial askew divisions per root
ns
***
****
**
Col-0
irk-1
irk-4
G
pIRK:IRK-GFP, irk-4
pIRK:IRKΔK-GFP, irk-4
H
Periclinal
Radial askew
Endodermal periclinal divisions per root
Endodermal radial askew divisions per root
Col-0
IRK, irk-4
IRKΔK, irk-4

Figure 1. Arabidopsis root cellular organization, cell division plane orientations and *irk* phenotype. (A) Schematic of a root tip (left) with endodermal cell files highlighted in gray. (Center) Close ups of median longitudinal and (right) transverse sections with transverse anticlinal (green), longitudinal anticlinal (cyan), periclinal (magenta), and radial askew (orange) endodermal divisions indicated by dotted lines. (B) Schematic of ground tissue formation from initial cell division to middle cortex formation. (C) The different division orientations are also shown in schematics of single endodermal cells represented as cubes. (D) Confocal micrographs of a portion of the root tip showing the median longitudinal section (left) and transverse section (right) with endodermal cells that have undergone one of the defined divisions highlighted. Please note that transverse anticlinal divisions are not visible in the transverse axis and longitudinal anticlinal divisions are not visible in the longitudinal axis. (E) Confocal micrographs showing transverse sections (upper) and median longitudinal sections (lower) of Col-0, *irk-1*, and *irk-4* root tips stained with PI (grey) with abnormal cell divisions indicated by arrowheads colored as described above. (F) Quantification of total number of periclinal and radial askew divisions per genotype (n = 35-40 roots per genotype). Graphs show the combined results from 3 independent replicates. (G) Confocal micrographs showing transverse sections (upper) and median longitudinal sections (lower) of *irk-4* expressing (left) *pIRK:IRK-GFP* and (right) *pIRK:IRK∆K-GFP* stained with PI (grey) merged with GFP (green). (F) Quantification of total number of periclinal and radial askew divisions in each genotype (n = 25 roots per genotype). Graphs show the combined results from 2 independent replicates. Statistics: P-values are indicated by asterisks *($p \leq 0.05$), **($p \leq 0.01$), ***($p \leq 0.001$), ****($p \leq 0.0001$), and NS (not significantly different) as determined by a one-way ANOVA using Dunn's multiple comparison test. Scale bars: 50 µm.

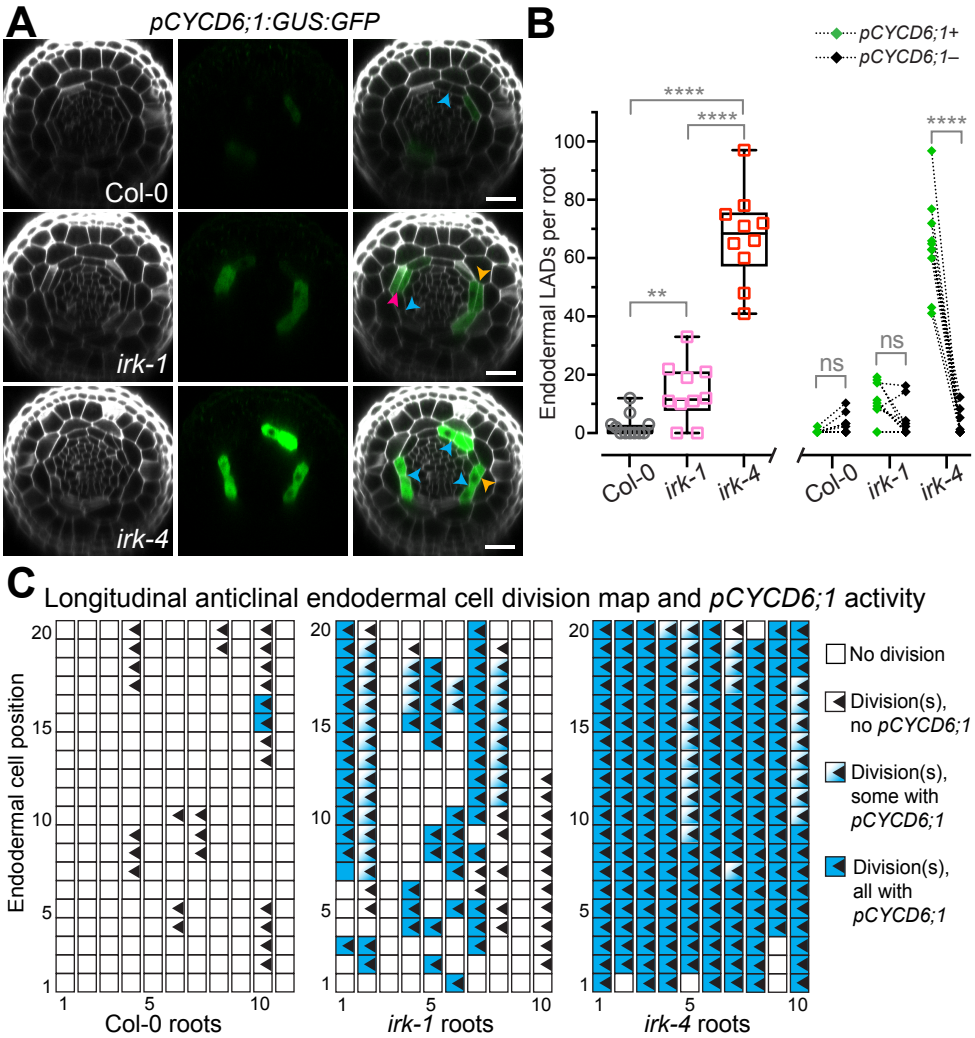

Figure 2. Longitudinal anticlinal endodermal cell divisions show *pCYCD6;1* activity most often in *irk* mutants. (A) Confocal micrographs of transverse optical sections of Arabidopsis root meristems at endodermal cell position 10 (ED10). Roots of each genotype expressing *pCYCD6;1:GUS:GFP* were stained with propidium iodide (PI, grey, right panels) to visualize cells and *pCYCD6;1* activity (erGFP, green, center panels) and the merged images (right panels). Endodermal division orientations: periclinal (magenta arrowhead), longitudinal anticlinal (cyan arrowhead), and radial askew (orange arrowhead). Scale bar = 50 µm. (B) Quantification of endodermal longitudinal anticlinal divisions (LADS) per root. (B) Box plot showing total number of LADs per root with whiskers indicating min/max with interquartile range and median shown with black boxes/lines, respectively, and colored symbols show measurements for individual roots. (C) Point graph showing the number of LADs with (+) *pCYCD6;1* activity (green diamond) or without (–) *pCYCD6;1* activity (black diamond). (D) Cell division map for LADs in the first 20 endodermal cell above the QC (n = 10-11 roots per genotype, the same roots were analyzed in B-D). Data shown are from a single representative biological replicate of ≥2, with similar results. Statistics: ns = not significantly different, p values: ** < 0.01, **** < 0.0001, assayed by Mann-Whitney tests.

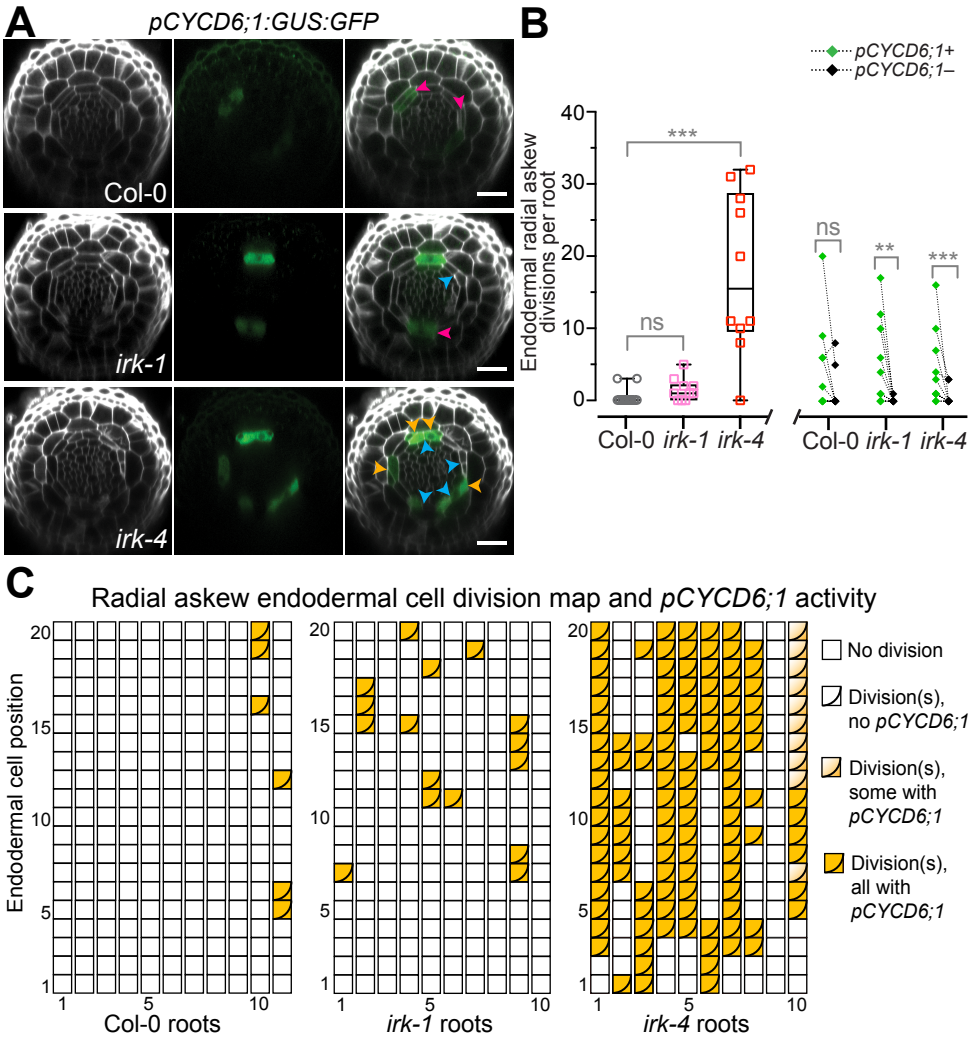

Figure 3. Radial askew endodermal divisions consistently show *pCYCD6;1* activity. (A) Confocal micrographs of transverse optical sections of Arabidopsis root meristems at endodermal cell position 10 (ED10). Roots of each genotype expressing *pCYCD6;1:GUS:GFP* were stained with propidium iodide (PI, grey, right panels) to visualize cells and *pCYCD6;1* activity (erGFP, green, center panels) and the merged images (right panels). Endodermal cell division orientation as indicated in previous figures. Scale bar = 50 µm. (B) Quantification of radial askew endodermal divisions per root (the same roots as in Figure 2). Box plot showing total number divisions per root with whiskers indicating min/max with interquartile range and median shown with black boxes/lines, respectively, and colored symbols show measurements for individual roots. Point graph showing the number of radial askew divisions with (+) *pCYCD6;1* activity (green diamond) or without (–) *pCYCD6;1* activity (black diamond). (C) Endodermal cell division map for radial askew divisions in the first 20 endodermal cell above the QC (n = 10-11 roots per genotype, the same roots were analyzed in B-D). Data shown are from a single representative biological replicate of ≥2, with similar results. Statistics: ns = not significantly different, p values: * < 0.05, *** < 0.001, **** < 0.0001, assayed by Mann-Whitney tests.

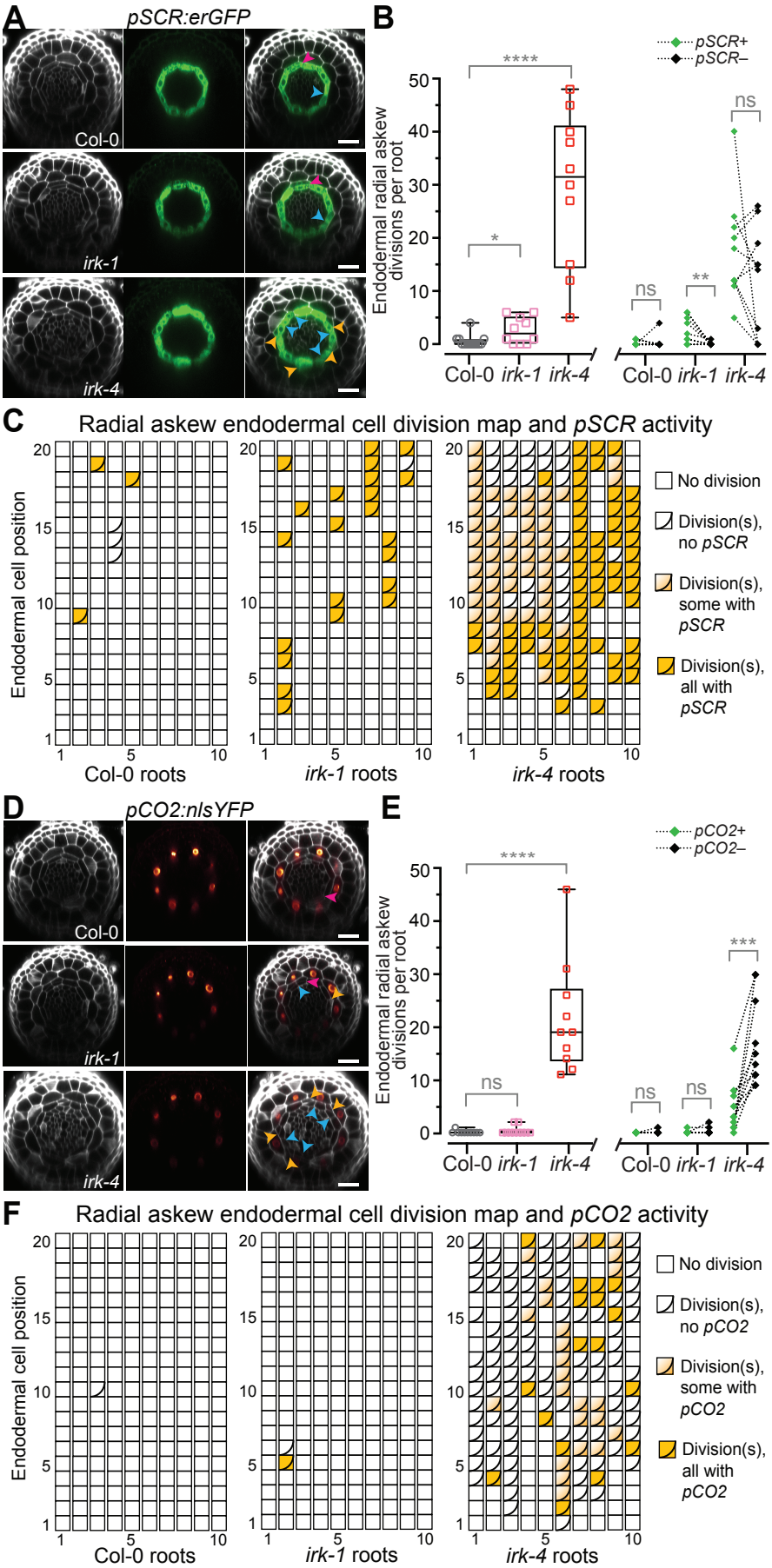
A
pSCR:erGFP
Col-0
irk-1
irk-4
B
pSCR+
pSCR–
Endodermal radial askew divisions per root
****
*
ns
**
ns
Col-0 irk-1 irk-4
Col-0 irk-1 irk-4
C
Radial askew endodermal cell division map and pSCR activity
Endodermal cell position
Col-0 roots
irk-1 roots
irk-4 roots
No division
Division(s), no pSCR
Division(s), some with pSCR
Division(s), all with pSCR
D
pCO2:nlsYFP
Col-0
irk-1
irk-4
E
pCO2+
pCO2–
Endodermal radial askew divisions per root
****
ns
ns
ns
***
Col-0 irk-1 irk-4
Col-0 irk-1 irk-4
F
Radial askew endodermal cell division map and pCO2 activity
Endodermal cell position
Col-0 roots
irk-1 roots
irk-4 roots
No division
Division(s), no pCO2
Division(s), some with pCO2
Division(s), all with pCO2

Figure 4. Radial askew division daughters show cell fate transition. (A, D) Confocal micrographs of transverse optical sections of Arabidopsis root meristems at endodermal cell position 10. Endodermal division orientations: periclinal (magenta arrowhead), longitudinal anticlinal (cyan arrowhead), and radial askew (orange arrowhead). Scale bar = X µm. (A) Roots of each genotype expressing *pSCR:erGFP* were stained with propidium iodide (PI, grey, right panels) to visualize cells, *pSCR* activity (erGFP, green, center panels), and the merged images (right panels). (B) Quantification of radial askew divisions per root and the numbers of radial askew divisions with or without *pSCR* activity. (C) Endodermal cell division map for radial askew divisions (n = 10 roots per genotype). (D) Roots of each genotype expressing *pCO2:nlsYFP* were stained with propidium iodide (PI, grey, right panels) to visualize cells and *pCO2* activity (nlsYFP red-yellow intensity gradient, center panels) and the merged images (right panels). (E) Quantification of radial askew divisions per root and the numbers of radial askew divisions with or without *pCO2* activity. (F) Endodermal cell division map for radial askew divisions (n = 10 roots per genotype). Box plots show total number of radial askew endodermal divisions per root with whiskers indicating min/max with interquartile range and median shown with black boxes/lines, respectively, and colored symbols show measurements for individual roots. Point graphs showing the number of radial askew divisions with (+) *pSCR/pCO2* activity (green diamond) or without (–) *pSCR/pCO2* activity (black diamond). Data shown are from a single representative biological replicate of ≥2, with similar results. Statistics: ns = not significantly different, p values: ** < 0.01, **** < 0.0001, assayed by Mann-Whitney tests.

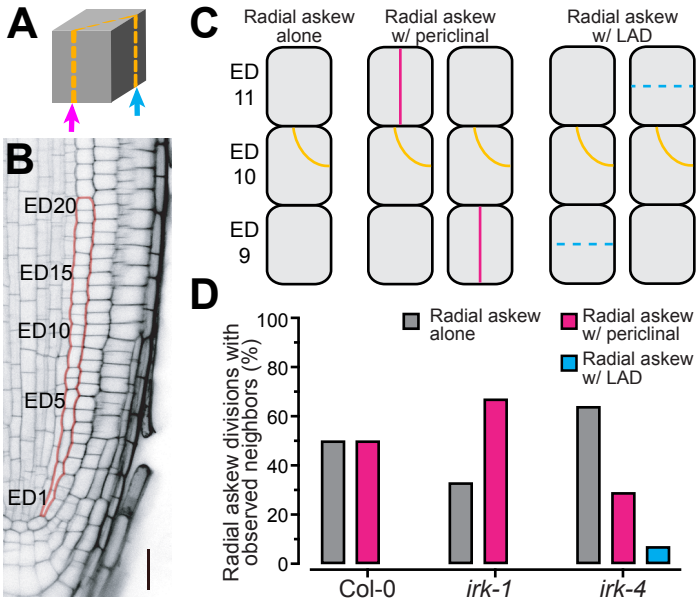

Figure 5. Radial askew endodermal divisions co-occur with periclinal divisions. (A) Single endodermal cell represented as a cube with radial askew division (orange dotted line) showing the attachment of the new cell plate at adjacent endodermal cell faces that are shared with periclinal (magenta arrow) and longitudinal anticlinal (cyan arrow) divisions, respectively. (B) Confocal micrograph of a median longitudinal section of a wild type root meristem stained with PI. Red outline indicates first 20 endodermal cells (ED1-20) above the QC. Scale bar = 50 µm. (C) Diagrams showing part of an endodermal cell file with a radial askew division (orange) neighbored by cells that have not divided or by neighboring cells that have undergone a periclinal (magenta line) or longitudinal anticlinal division (LAD, cyan dashed line as these divisions are not visible in the longitudinal axis). (D) Bar graph showing the proportion of radial askew divisions observed for each of the neighboring cell states (as in B) in Col-0, *irk-1* and *irk-4* roots expressing *pCYCD6;1:erGFP*. See methods section for additional details.

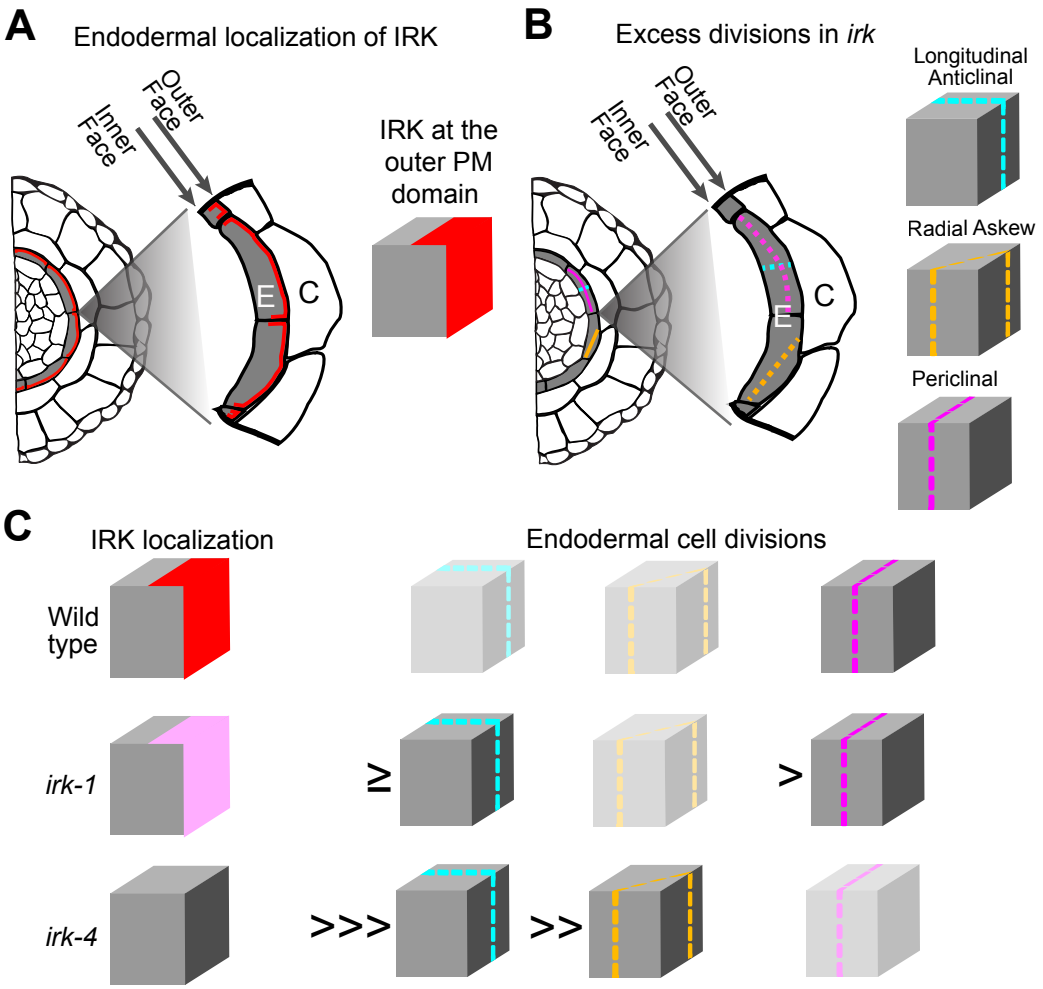

Figure 6. Schematics of IRK polar localization and excess endodermal divisions in *irk*. (A) Schematics of IRK-GFP polar localization (red lines) at the outer lateral endodermal cell face and (B) excess longitudinal anticlinal, radial askew, and periclinal divisions in *irk* (cyan, orange, and magenta lines, respectively). (C) Schematics of single endodermal cells, represented as cubes, showing IRK-GFP polarity and endodermal division phenotypes in the various IRK genotypes. The greater-than sign and the greater-than-or-equal-to sign indicate the extent to which the divisions are present in each genotype compared to Wild type. The lighter colored divisions are not different from Wild type. The excess endodermal cell divisions in *irk-4* are oriented such that one edge of the division plane contacts the endodermal cell face where IRK resides in Wild type, *irk-1*, and *irk-4* expressing IRKΔK-GFP.

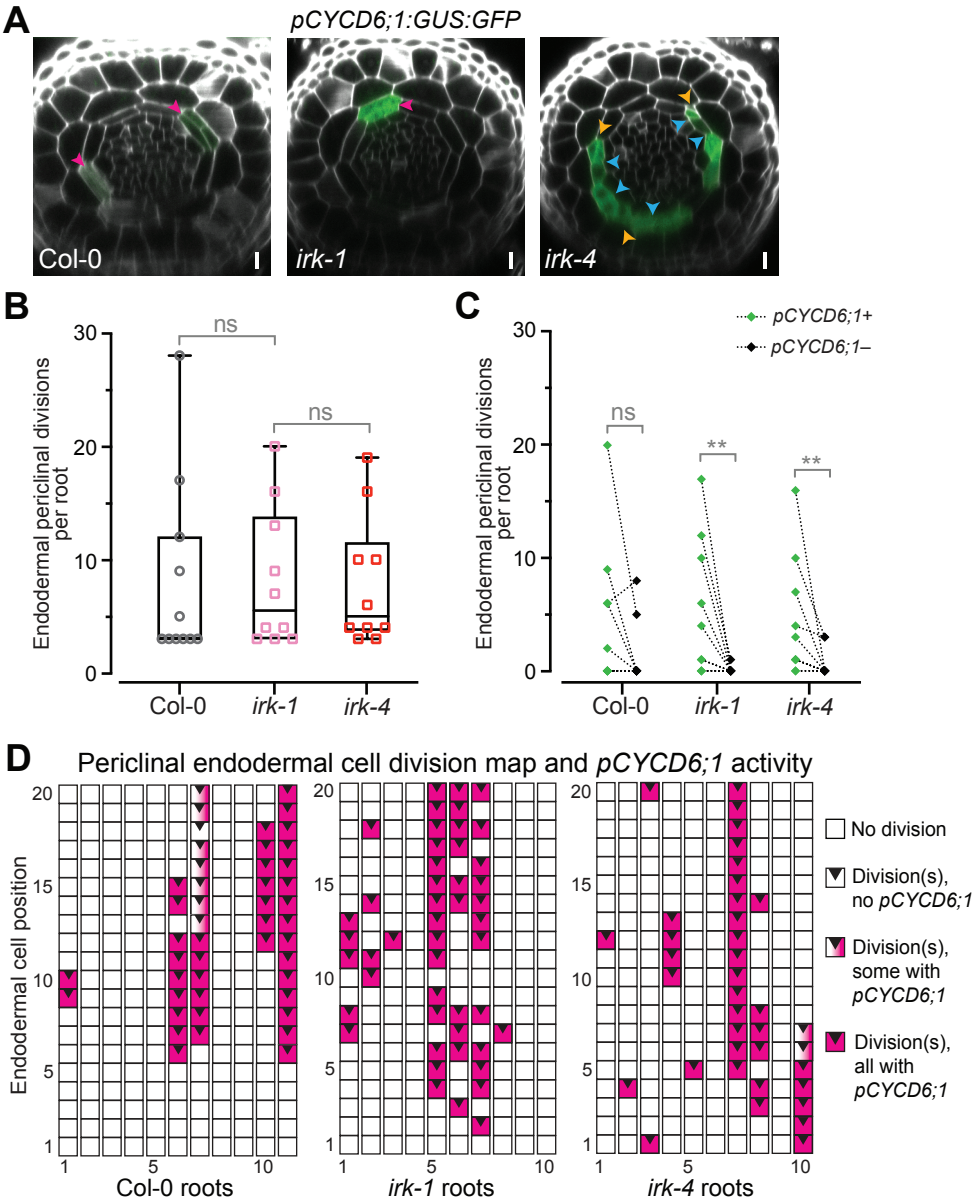

Figure S1. Most periclinal divisions are associated with *pCYCD6;1* activity. (A) Confocal micrographs of transverse optical sections of Arabidopsis root meristems expressing the *pCYCD6;1:GUS:GFP* transcriptional reporter. Optical sections acquired at endodermal cell position 10 and images show PI channel (gray) merged with GFP (green). Scale bar = 20μm. (B) Box plot showing total number of periclinal divisions per root with whiskers indicating min/max with interquartile range and median shown with black boxes/lines, respectively, and colored symbols show measurements for individual roots. (C) Point graph showing the number of divisions with (+) *pCYCD6;1* activity (green diamond) or without (–) *pCYCD6;1* activity (black diamond). (D) Cell division map for periclinal divisions in the first 20 endodermal cell above the QC (n = 10-11 roots per genotype, the same roots were analyzed in Figure 3). Data shown are from a single representative biological replicate of ≥2, with similar results. Statistics: ns = not significant, p values: * < 0.05, *** < 0.001, **** < 0.0001, assayed by Mann-Whitney test.

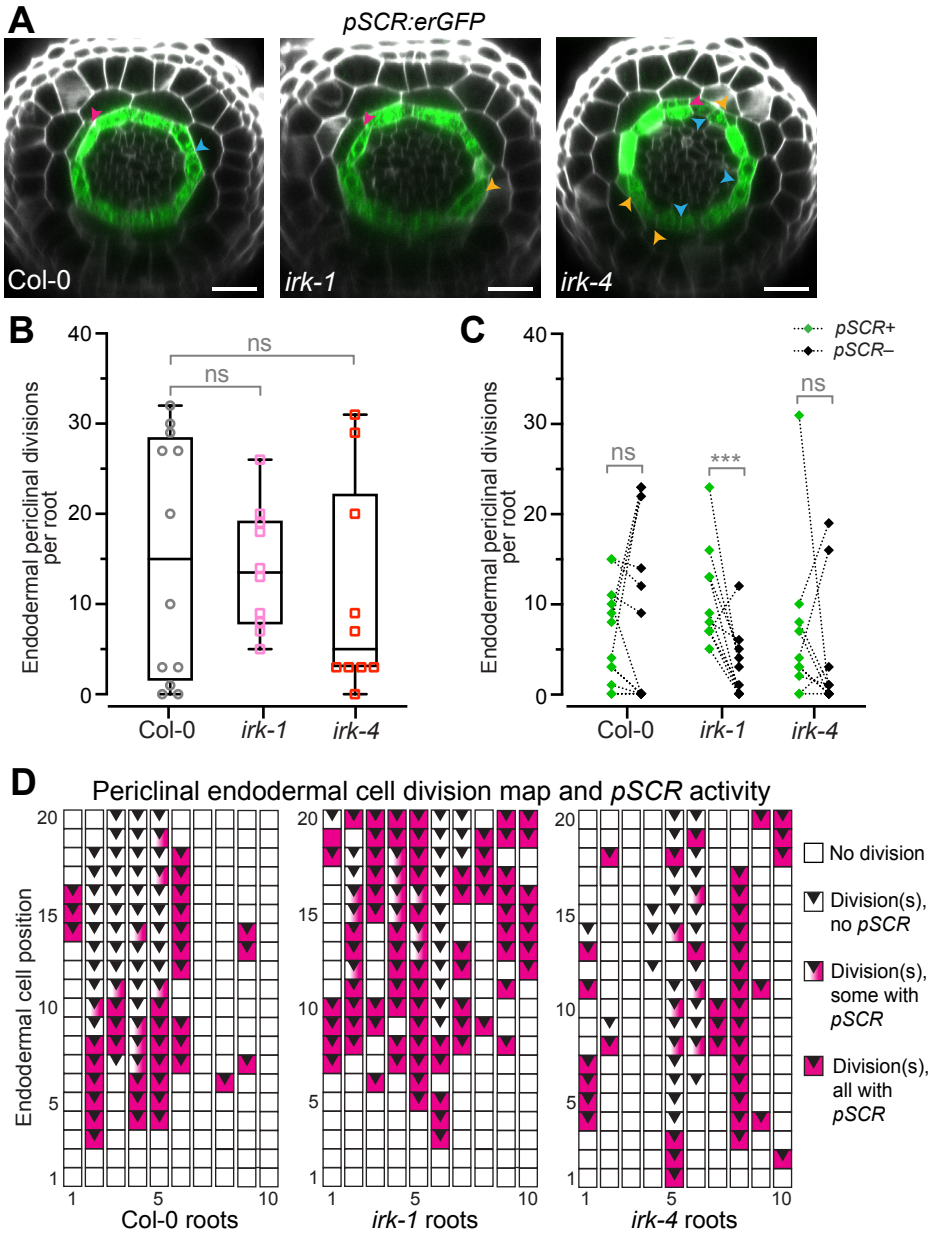

Figure S2. Periclinal endodermal division daughter cells often exhibit *pSCR* activity. (A) Confocal micrographs of transverse optical sections of Arabidopsis root meristems expressing the *pSCR:erGFP* transcriptional reporter. Optical sections acquired at endodermal cell position 10 and images show PI channel (gray) merged with GFP (green). Scale bar = 50 µm. (B) Box plot showing total number of periclinal divisions per root with whiskers indicating min/max with interquartile range and median shown with black boxes/lines, respectively, and colored symbols show measurements for individual roots. (C) Point graph showing the number of divisions with (+) *pSCR* activity (green diamond) or without (–) *pSCR* activity (black diamond). (D) Cell division map for periclinal divisions in the first 20 endodermal cell above the QC (n = 10 roots per genotype, the same roots were analyzed in Figure 4). Data shown are from a single representative biological replicate of ≥2, with similar results. Statistics: ns = not significant, p values: *** < 0.001, as assayed by Mann-Whitney test.

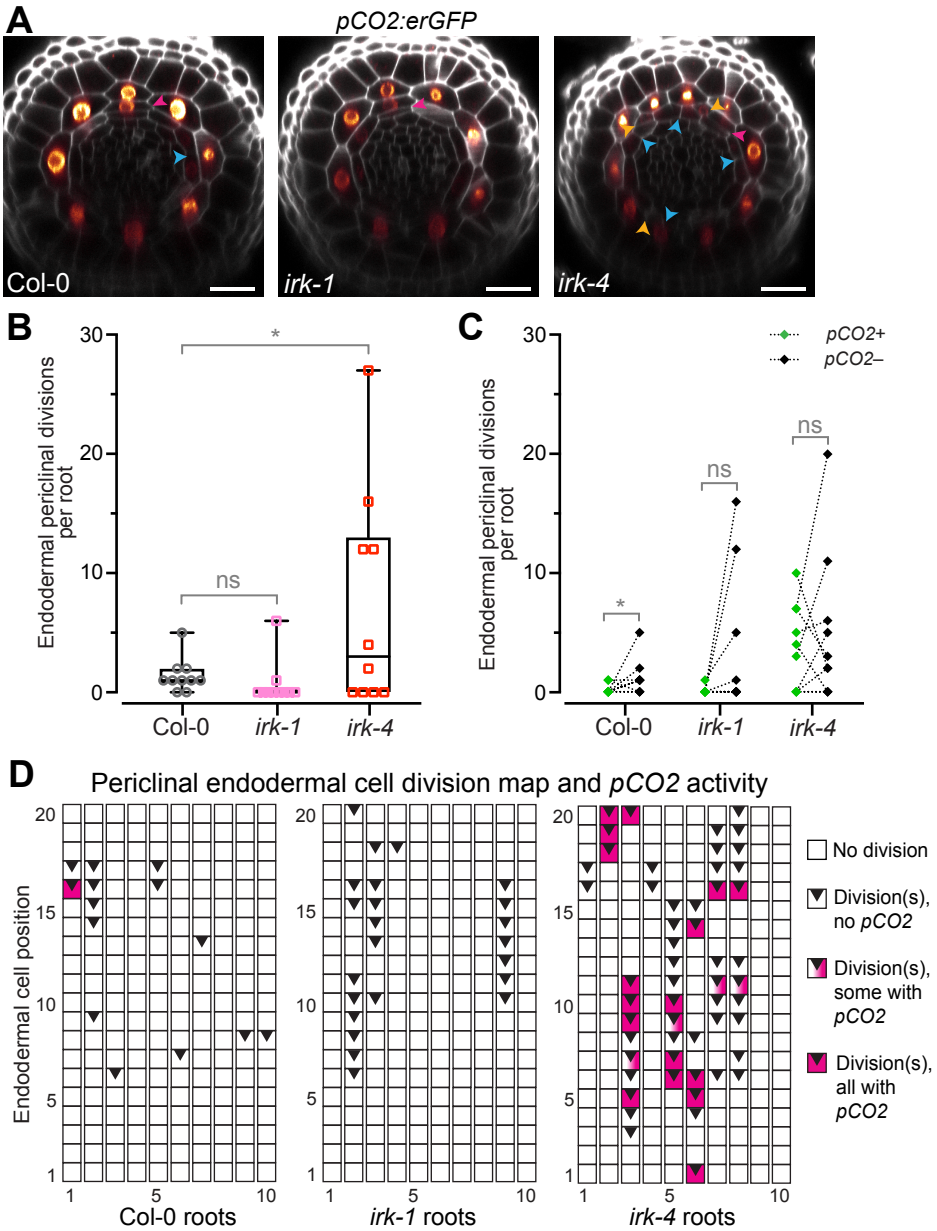

Figure 3S. Most periclinal endodermal division daughter cells do not show *pCO2* activity. (A) Confocal micrographs of transverse optical sections of Arabidopsis root meristems expressing the *pCO2:erGFP* transcriptional reporter. Optical sections acquired at endodermal cell position 10 and images show PI channel (gray) merged with YFP (yellow). Scale bar = 50 µm. (B) Box plot showing total number of periclinal divisions per root with whiskers indicating min/max with interquartile range and median shown with black boxes/lines, respectively, and colored symbols show measurements for individual roots. (C) Point graph showing the number of divisions with (+) *pCO2* activity (green diamond) or without (–) *pCO2* activity (black diamond). (D) Cell division map for periclinal divisions in the first 20 endodermal cell above the QC (n = 10 roots per genotype, the same roots were analyzed in Figure 4). Data shown are from a single representative biological replicate of ≥2, with similar results.Statistics: ns = not significant, p values: * < 0.05, assayed by the Mann-Whitney test.